Arch. Metall. Mater. **63** (2018), 3, 1329-1337

DOI: 10.24425/123808

A. GARBACZ-KLEMPKA*#, J.S. SUCHY*, Z. KWAK*, P. DŁUGOSZ**, T. STOLARCZYK***

CASTING TECHNOLOGY EXPERIMENT AND COMPUTER MODELING OF ORNAMENTS FROM BRONZE AGE

The casting workshop was discovered with numerous artifacts, confirming the existence of the manufacturing process of metal ornaments using ceramic molds and investment casting technology in Lower Silesia (Poland) in 7-6 BC. The research has yielded significant technological information about the bronze casting field, especially the alloys that were used and the artifacts that were made from them.

Based on the analyses, the model alloys were experimentally reconstructed. Taking advantage of the computer-modeling method, a geometric visualization of the bronze bracelets was performed; subsequently, we simulated pouring liquid metal in the ceramic molds and observed the alloy solidification. These steps made it possible to better understand the casting processes from the perspective of the mold technology as well as the melting and casting of alloys.

Keywords: Archeometallurgy, Copper Alloys, Investment Casting Technology, Lost-Wax Casting, Modeling

1. Introduction

Knowledge of the casting technology and metalworking of a historical civilization is confirmed from the archeological artifacts to which they belong, the casting molds, metals, tools, and ornaments found in old foundry workshops, and the metallurgical graves or metallurgical hoards found at archeological sites [1-4].

Skill and improvement of the investment casting technique was important in the progress of casting technology engineering [1]. This method of precision casting is one of the principal manufacturing methods applied contemporarily in the medical, automotive, aeronautical, and arms industries as well as in the areas of jewelry casting and art [3-12].

In the Bronze Age, clay molds helped people create small and bigger ornaments by the lost-wax casting method. Bracelets, rings, pins, and torques were made in this way.

The workshop in Lower Silesia (Grzybiany settlement) was functioning in Poland dating back to the Hallstatt C period (from the seventh to mid-sixth century BC), which indicates good knowledge in this period of lost-wax casting [2,13]. In this settlement, ceramic casting molds were found that have been assessed to be the biggest collection of molds for bracelet and necklace manufacturing from the Bronze Age in Poland [13].

A group of casting molds and metal ornaments from the Grzybiany settlement was investigated. The artifacts was submitted to macro-and micro-scopic analyses, observations, chemical composition assessment, and X-ray imaging [13-15].

Previous investigations and experiences in workshop casting from Bronze Age research [13] were utilized in order to reconstruct the applied technology, in the experimental form as well as in the computer modeling of the casting processes.

Analytical methods [16-21] and computer modeling processes are important for archeology and cultural heritage research. They are increasingly used to recognize and reproduce the primeval casting processes and metalworking [22-26].

2. Methodology and research

Using the performed micro- and macro-scopic investigations, X-Ray imaging, and chemical composition analyses , the experiments of recreating model alloys and technology reconstruction by means of the computer modeling methods were performed [13].

The experiment of recreating the model alloys was carried out by successively adding pure metals into copper. The ingredients were melted in the laboratory furnace using a charcoal cover and were cast into the ceramic molds. Thermal analysis was conducted during the melting and solidifying of the cast in the mold. The cast alloys were analyzed with respect to their microstructures and chemical contents.

By the visualization of 3D models, the molds and casts were prepared based on physicochemical and structural tests in order to simulate the casting and solidifying in the mold. Three-dimensional models were created using the SolidWorks program,

* AGH UNIVERSITY OF SCIENCE AND TECHNOLOGY, FACULTY OF FOUNDRY ENGINEERING, HISTORICAL LAYERS RESEARCH CENTER, REYMONTA 23 STR., 30-059 KRAKOW, POLAND
** FOUNDRY RESEARCH INSTITUTE, ZAKOPIAŃSKA 73 STR, 30-418 KRAKOW, POLAND
*** COPPER MUSEUM, PARTYZANTÓW 3 STR., 59-220 LEGNICA, POLAND

Corresponding author: agarbacz@agh.edu.pl

while the simulations were performed using Magma[5] software. Due to the lack of data, the nearest parameter values (but not identical ones) were accepted, such as the chemical composition of the alloys, mold materials, or casting temperatures.

2.1. Study of chemical composition of bracelets

In the group of Grzybiany artifacts, there are relatively few whole bracelets (which, incidentally, do not match the researched casting molds). Therefore, the rods and wires that could have been parts of the bracelets before they were damaged were also considered to be the part of this group. The studied bracelets and their fragments were cast from copper matrix alloys, which significantly differed in their alloying component proportions and tramp elements.

An unadorned bracelet with a circular cross section was made of a two-component tin bronze of the Cu-Sn type, with the slight addition of lead (inv. no. 10/78) (Fig. 1a). A partially preserved bracelet manufactured from a twisted flat bar was made of a tin bronze of the Cu-Sn type, with a 1% addition of lead (bracelet inv. no. 300/79) (Fig. 1b). A thin cast rod (maybe a fragment or a semi-finished product intended for bracelet making) was made of a three-component bronze of the Cu-Pb-Sn type, with more lead than tin (rod inv. no. 22/2010) (Fig. 1c). Another bracelet fragment contains mainly copper and natural impurities such as silver, antimony, and arsenic. On the surface, some remains of the burnt clay mold were registered along with the slag inclusions in its structure and on its surface. (rod with slag inv. no. 10/71) (Fig. 2a). The research of an unadorned bracelet fragment with a circular cross section and visible fracture (bracelet rod inv. no. 47/2010) (Fig. 2b) showed that it was cast from lead bronze of the Cu-Pb type with a significant number of additives (6% Sb, 2.5% As, 2.4% Ni, and others). An unadorned rod with a circular cross section was part of a bracelet or necklace (bracelet part inv. no. CL6568) (Fig. 3); it was cast from tin-lead bronze (Cu-Sn-Pb) with a share of antimony, arsenic, and silver. The chemical profile of the described bracelets and broken elements that could have been parts of bracelets or necklaces is collected in the table (Table 1).

Fig. 1. Bracelet fragments: single coil bracelet with circular cross-section (a); ornamented bracelet (b); rod (c)

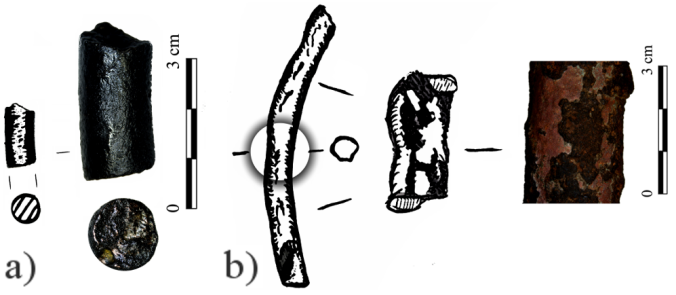

Fig. 2. Rod fragments: rod with slag own graphic design based on (a); rod own graphic design based on (b)

Fig. 3. Rot fragment with the views of both ends according to technical drawing

2.2. Model alloys for chosen historical metal artifacts

The rod fragment with a circular cross-section (inv. no. 47/2010) may be a part of a bracelet or a necklace (Fig. 2b), suggesting that the applied material was of a high inhomogeneity of structure and high brittleness. Supposedly, this is an element of a necklace that was cast in a ceramic mold with a diameter of about 10mm. One studied element with a chemical content of 32% Pb, 5.8% Sb, 2.5% As, 2.4% Ni, 1% Fe, and 54.3% Cu (Table 2) stands out because of its metallic color of bright copper and metallic luster. It is characterized by high porosity at the

TABLE 1

Chemical composition of bracelet and rod samples from Grzybiany, as determined with energy-dispersive XRF (Wt. %)

Nr	Object	Inv. no.	Fe	Co	Ni	Cu	Zn	As	Ag	Sn	Sb	Pb	Bi
1	Rod with slag	10/71	0.17	0.07	0.19	97.34	0.12	0.25	0.9	0.01	0.86	0.09	0.01
2	Bracelet fragment with a clasp	14/72	1.01	0.08	0.21	81.74	0.10	0.57	0.10	15.02	0.44	0.69	0.04
3	Bracelet	434/77	1.39	0.11	0.51	74.84	0.13	0.82	0.48	19.16	0.97	1.54	0.05
4	One-coil bracelet	10/78	0.41	0.07	0.16	84.78	0.14	0.28	0.04	13.56	0.09	0.43	0.04
5	Ornamented bracelet	300/79	0.73	0.13	0.4	87.66	0.05	0.43	0.16	8.57	0.75	1.09	0.03
6	Ornamented bracelet	107/80	1.89	0.08	0.45	83.40	0.12	0.51	0.31	9.95	0.9	2.33	0.15
7	Rod	22/2010	0.03	0.10	0.15	60.56	0.11	0.25	0.27	10.01	0.67	27.7	0.15
8	Rod	47/2010	1.01	0.98	2.43	54.31	0.13	2.53	0.66	0.01	5.86	31.95	0.14
9	Bracelet fragment	CL6568	0.23	0.09	0.23	80.41	0.11	0.48	0.72	13.00	2.47	2.21	0.05

fracture. The fracture is brittle, coarse-grained, and inhomogeneous. In the microstructure of the studied element, a dendritic character of the crystallites structure is noticeable, with numerous white irregular precipitates spaced within the whole volume of the artifact (Fig. 4). Dendritic crystallites are darker and can be identified with the copper matrix, whereas the white phases are not homogeneous; they contain a mixture of phases on the lead matrix and other low-melting elements. The inhomogeneity of these light sections is especially visible at high magnifications.

TABLE 2

Temperature of phase changes of GST3 alloy – CuPb32Sb6Fe1As2Ni2

GST3 Alloy Temp	T_1	T_2	T_3	T_4	T_5
°C	1085	985	895	668	327

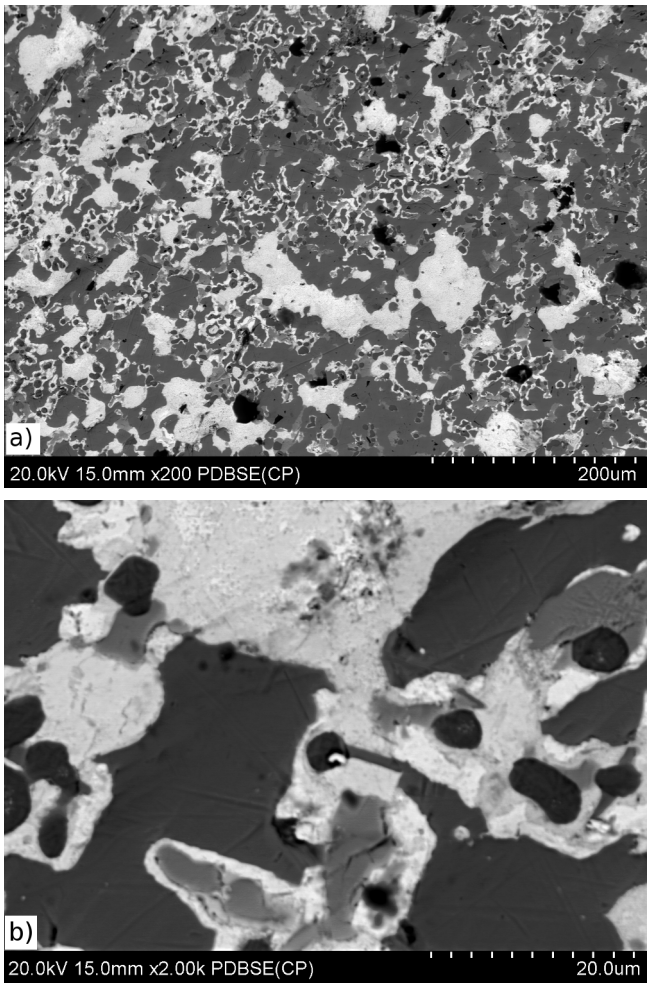

Fig. 4. SEM picture. Rod fragment microstructure: 200× (a), 2000× (b)

Further research was conducted using a scanning electron microscope with energy-dispersive X-ray spectroscopy in the micro-areas (SEM-EDS). This showed the presence of copper that formed large dendrites of a solid solution, including additions of lead, silver, arsenic, and antimony. Dark precipitates in the area of the dendritic copper crystallites were identified as sulfur inclusions.

The model alloy, recreated for this historical artifact (GST3 – CuPb32Sb6Fe1As2Ni2), was subjected to tests. Thermal analysis results (Fig. 5), (Table 3) show that the alloy containing 32% lead solidifies within a very broad temperature range, from 668° to 327°C (T4-T5). The beginning of solidification (T1) determined at 1085°C is related to the peritectic reaction from the Cu-Fe equilibrium (taking place at high temperatures) in connection with the iron presence in the alloy. Subsequently, crystallization of the dendrites of the solid solutions of antimony and arsenic in copper at 985°C (T2) with a transition at a temperature of 895°C (T3) and a eutectic transition – at 668°C (T4) – of the phases containing antimony, arsenic, and lead Sb-As-Pb. The solidification process finishes with the effects of the heat emission at a temperature of 327°C (T5), which corresponds to the crystallization temperature of pure lead.

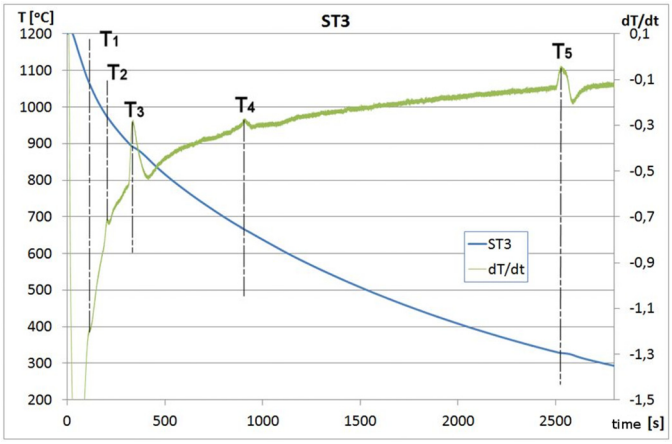

Fig. 5. TA and ADT analysis curves for GST3 alloy – CuPb32Sb6Fe1As2Ni2

TABLE 3

Chosen technological parameters for MAGMA[5] software simulation program of bracelets based on mold from Grzybiany

Version of simulation	Artefact visualisation based on mould inv. no.	Description	Mould temerature /°C	Alloy	Pouring temperature /°C
1	182/77	Sprue as in radioscopic picture	20	CuSn5ZnPb	1100
2	14/78	Using longer sprue and greater inlet	25	CuSn12	1100
3			300		
4			600		
5	14/78	Sprue as in radioscopic picture	600	CuSn12	1100
6			700		
7			800		

The characteristic microstructure for the recreated GST3 alloy is presented in the picture (Fig. 6). The similarity between the microstructure of the recreated and original alloy (Fig. 4) proves that the experiment of reconstructing the casting and

solidification process of the archeological alloy was conducted in the correct way (inv. no. 47/2010).

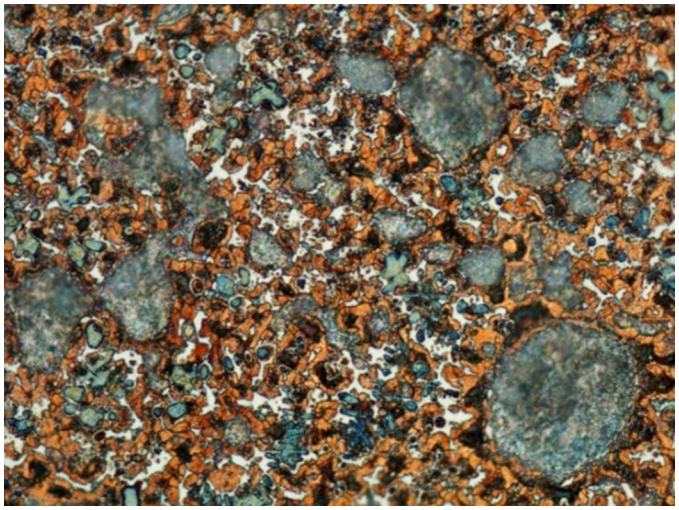

Fig. 6. Microstructure of the model GST alloy – CuPb32Sb6Fe1As2Ni2, 500×

Another type of material (marked as GST4) was also recreated in the research according to the chemical composition of the metal rod (inv. no. 10/71), possibly a fragment of a bracelet or necklace. GST4 ideally should be pure copper, and the elements present in its structure are unwanted impurities. This type is represented by copper samples in the archeological finds are far from the GST4 purity due to the technological difficulties at the stage of extracting copper from its ore. During these metallurgical processes, the elements present in the ores remain in the raw copper material [1,5].

Observations were conducted of the surface (Fig. 7) and microstructure (Fig. 8) of the rod-shaped cast (inv. no. 10/71). On the one hand, the rod showed features of casting with a characteristic misrun defect, which resulted from a low temperature of the liquid metal during its pouring into a clay mold. This situation could have also been caused by the low castability of copper containing small amounts of alloy additions (in this cast, the elements point to both the origin and technology). On the other hand, the rod was covered by a layer of slag (hard and brittle), which probably got into the mold cavity and solidified there, blocking the metal flow. In the microstructure of the cross-section of rod, there is a visible dominant dark area of the slag with small, light fragments of metallic copper against the non-metallic structure of the slag (Fig. 8).

Fig. 7. Surface of copper rod, 50×

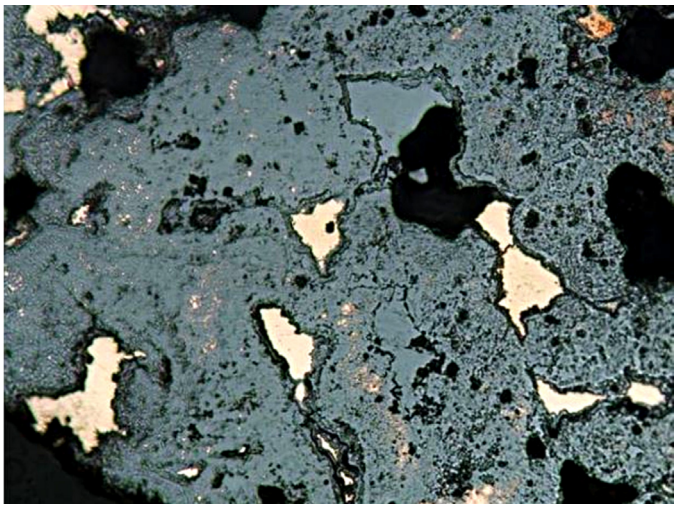

Fig. 8. Fragment of metal rod, microstructure, 100×

Model alloy GST4 containing 0.9% Ag, 0.9% Sb, 0.3% As, 0.2% Ni, and 0.2% Fe with 97.3% Cu (Table 2) solidifies in a typical way for copper with silver and a small amount of alloy additives at a temperature of about 1000°C with big, distinct dendrites being crystallized, showing slight heat effects at lower temperatures. The characteristic microstructure of GST4 copper is presented in the photograph (Fig. 9).

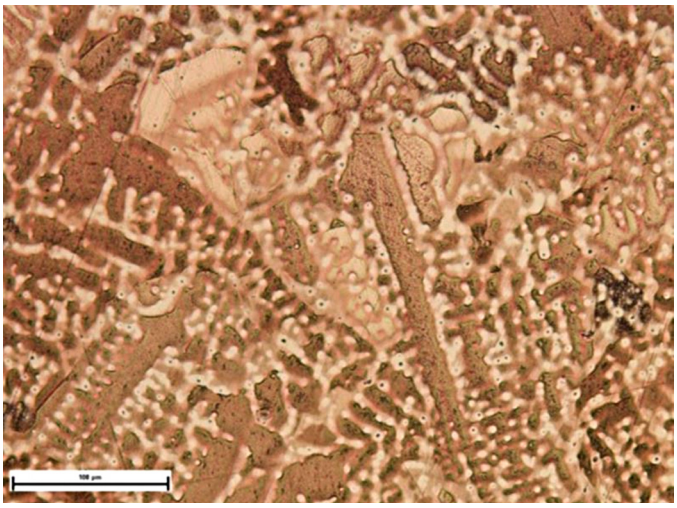

Fig. 9. Microstructure of model alloy GST4 – CuAg1Sb1As0.3, 500×

For the recreated experimental alloys, it is possible to conduct an analysis of the utility and technological properties like luster and color (Fig. 10), resistivity to corrosion, castability, hardness, plasticity, and strength.

Fig. 10. Model alloys GST1-GST4. Cross-sections of model alloy samples, for archeological copper alloys with different content of intentional alloy additions as well as elements connected with their origin and technology: 1 – GST1 – CuSn11; 2-GST2 – CuSn8Pb1As1Sb1Fe2Ni1; 3 – GST3 – CuPb32As2Sb6Fe1Ni2; 4- GST4 – CuAg1Sb1As0.3

2.3. X-ray radiography investigations of casting molds

Some of the molds from the Grzybiany workshop are preserved almost whole, except for the part of the main sprue together with the cup (inv. no. 14/78), making filling the mold possible. To determine the shape of the mold cavity, macroscopic observations were conducted as well as an X-ray radiography test [13,14]. Based on these, the molds were classified as intended for the casting of bracelets, necklaces, pins, and loops.

The cavity shape would be visible in the X-ray image of the mold used for casting bracelets with circular cross-sections. The main sprue (also with a circular cross section) is perpendicular to the surface of the bracelet. The sprue diameter is 6-8 mm.

Another mold for bracelet casting has a cavity cross-section in the shape of a letter C (inv. no. 182/77) (Figs. 11).

The remaining molds vary to a small extent with respect to the mold cavity shape and diameter of the cavity cross-section, which falls within a range of 4-11 mm. One bracelet or necklace mold stands out from the others because of its cross-section of the double roll shape. In the mold collection, there were also molds with a rhomboid cross-section intended for necklace casting. The visualization of the possible jewelry elements to be made in these molds is presented in Figures (Figs. 12-14).

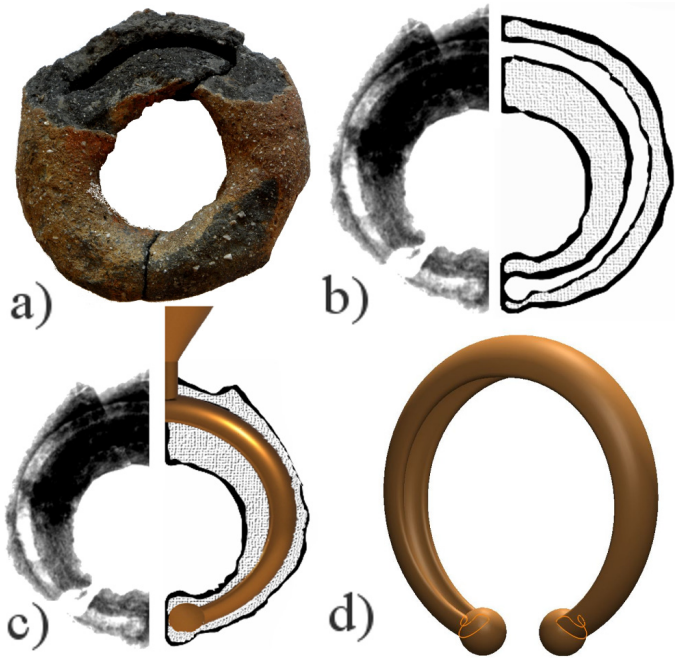

Fig. 11. Fragment of casting mold, inv. no. 182/77 (a); graphic documentation based on X-ray image (b); artifact visualization based on mold (c,d)

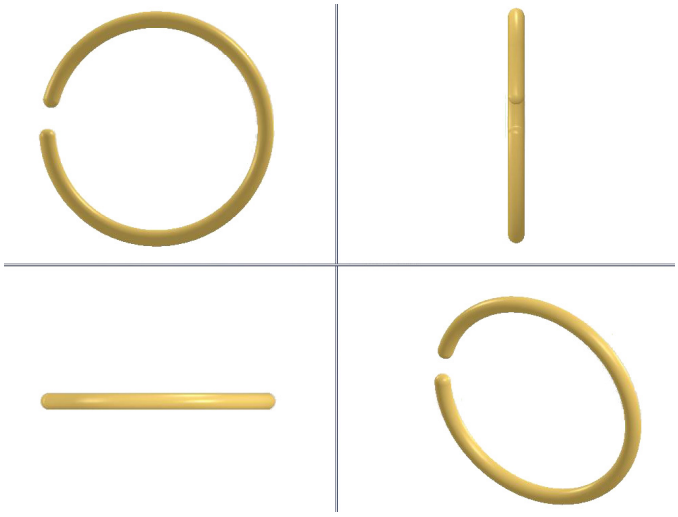

Fig. 12. Cast visualization based on radioscopic picture of artifact inv. no. 43/77

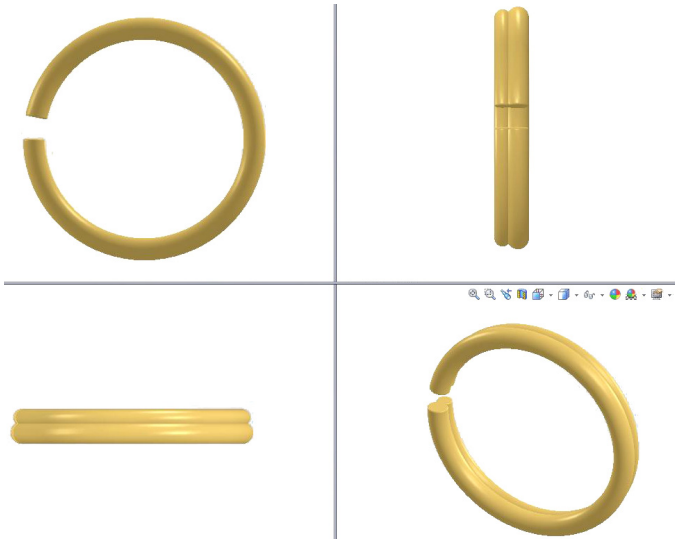

Fig. 13. Cast visualization based on ceramic mold part for artifact inv. no. 92/79

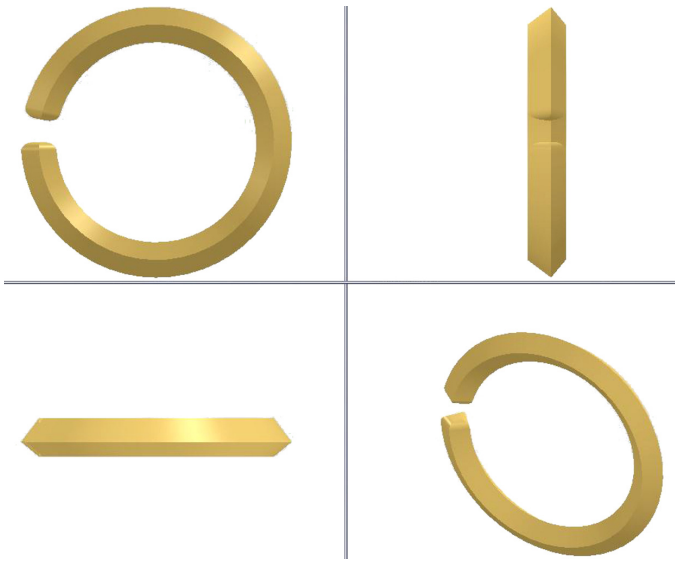

Fig. 14. Cast visualization based on picture of mold fragment for inv. no. 29/78 artifact

2.4. Computer reconstruction of models

A synthesis of the physicochemical and structural research results was conducted for the molds and metal artifacts in order to perform computer reconstruction of the casts. A 3D visualization made it possible to recreate the process of filling the molds with liquid metal and of the cast solidification. The results compile the visualization of the artifacts as well as the matching molds. Based on the mold cavity measurements and X-ray images, a graphic documentation of the molds was prepared, and the matching bracelets were reconstructed (Figs. 10, 15).

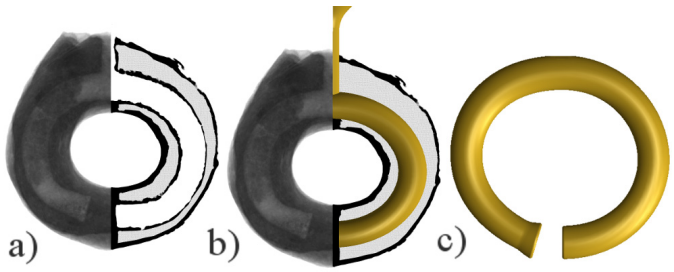

Fig. 15. Graphic documentation based on X-ray image of casting mold fragment (inv. no. 14/78) (a), artifact visualization based on mold (b,c)

Wax models and the matching molds were made by hand; therefore, their edges were not uniform, their proportions were not balanced, and the repeatability sometimes was only approximated. During further design stages (based on the 2D documentation and 3D for the bracelets), the three-dimensional models with the matching gating system (Figs. 16a, 17a) and the matching molds (Figs. 16b-d, 17b-d) were recreated using computer-aided design.

Owing to the design work conducted in the CAD environment, the casting molds were reconstructed, with their cavities corresponding to the radiologic pictures. Computer simulations

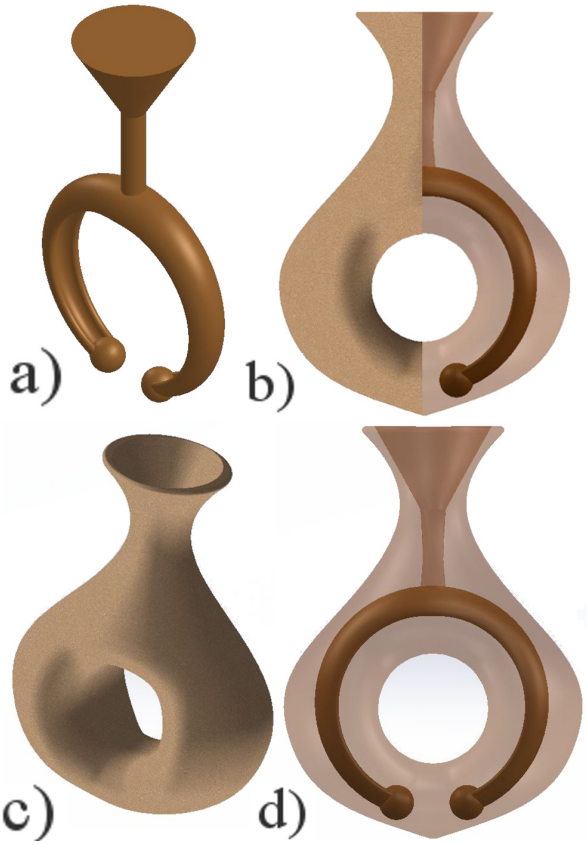

Fig. 16. Visualization of artifact inv.no. 182/77 connected with its gating system (a), virtual model placed in mold (b,d) and casting mold (c)

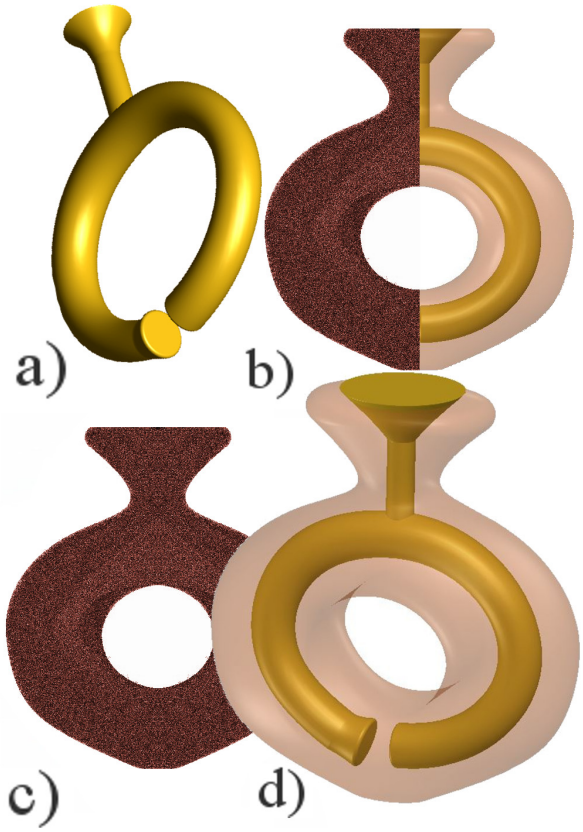

Fig. 17. Bronze bracelet visualization inv. no. 14/78, connected with its gating system (a), virtual picture of model placed in mold (b,d), and casting mold (c)

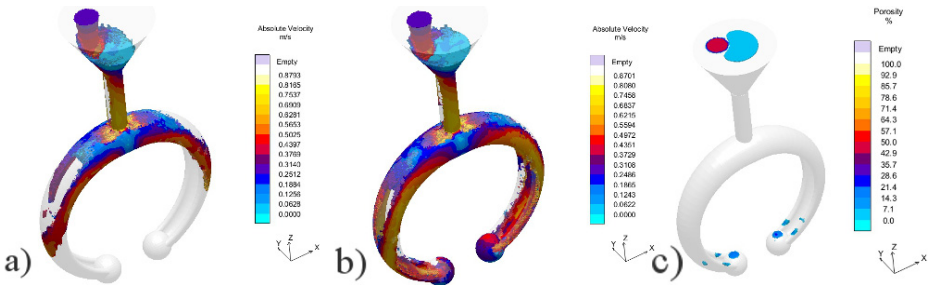

Fig. 18. Simulation for artifact inv. no. 182/77, using sprue with dimensions matching X-ray image: material speed characteristics after 302 ms since beginning of pouring (a), material speed characteristics after 458.9 ms since beginning of pouring (b), porosity distribution after 1 minute and 3 seconds since beginning of crystallization process (c)

of the filling of the molds were conducted, taking into account the technological parameters resulting from the analytical research; namely, the mold material and temperature, with the approximate recreation of the two- and three-component historical alloys.

To determine the role of the gating system for the reconstructed molds and the possibilities of using them for bracelet casting, the simulations were performed, applying various sizes of different elements of the gating system as well as using different mold temperatures (Table 3).

The results of the chosen simulations performed for artifacts inv. no. 182/77 and 14/78 using the CuSn5ZnPb and CuSn12 alloys are presented below (Fig. 18).

For the bracelet mold that is crescent-shaped in its cross section (inv. no. 182/770, (Fig. 18a-b), there is a number of factors pointed out in the simulation that lead to a possible porosity of the cast (Figs. 18c, 19). These are metal turbulences in the lower part of the bracelet, the highest solidifying temperatures in the same areas, shrinkage during metal cooling at a level of about 1.15%, and the fact that the bracelet solidifies in its thinnest sections first, thus cutting off the possibility of metal flow into the knobs at the end.

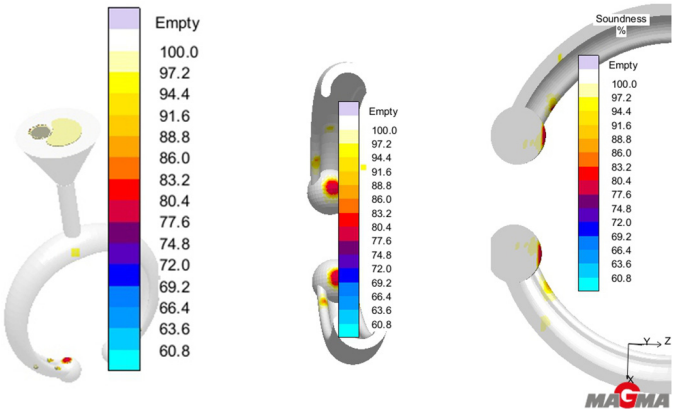

Fig. 19. Soundness when using main sprue with dimensions matching the X-ray image for artifact inv. no. 182/77 after 1 minute and 3 seconds form onset of crystallization

In the case of the bracelet with the asymmetric ending (inv. no. 14/78), the sprue was experimentally elongated, which resulted in deep porosity in the top part of the bracelet, appearing on the surface of the cast (Fig. 20). Therefore, the original gating system, recreated on the basis of the defectoscopic research of the mold, combined with heating the mold to 600°, 700°, and 800°C can introduce porosity into other regions of the cast and scatter its shape (Figs. 21-22).

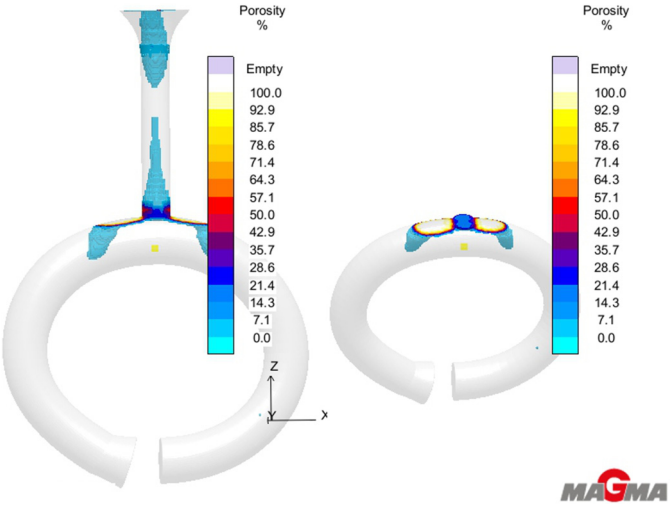

Fig. 20. Cast porosity when using elongated sprue for artifact inv. no. 14/78 after 2 minutes and 24 seconds since crystallization onset, mold heated to 300°C

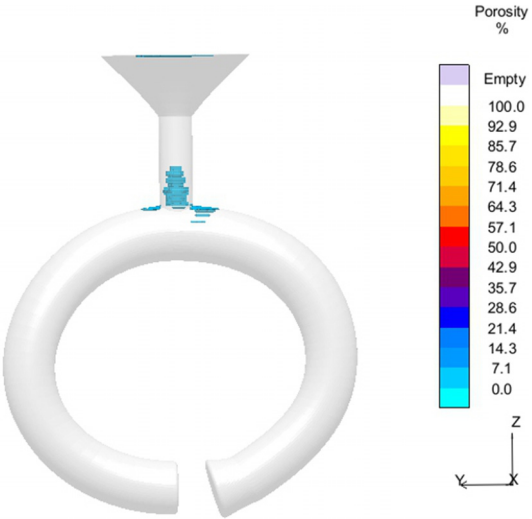

Fig. 21. Cast porosity using main sprue with dimensions matching radioscopic picture for artifact inv. no. 14/78 after 58 seconds from crystallization onset, mold heated to 600°C

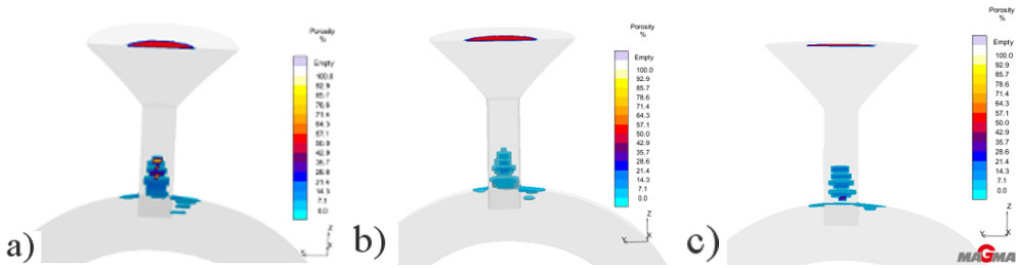

Fig. 22. Cast porosity using main sprue with dimensions matching the X-ray image for artifact inv. no. 14/78: mold heated to 600°C (a); mold heated to 700°C (b); mold heated to 800°C (c)

3. Conclusions

Based on the combined macroscopic, physicochemical, and defectoscopic tests, an attempt was undertaken to recreate alloys and casting technology of the metal ornaments. The models of the alloys were recreated in our laboratory experiment, with the application of modern engineering programs by means of virtual 3D models and simulations of the investment casting technology.

The selected characteristic casting alloys underwent the experiment of recreating the laboratory conditions on the basis of the chemical composition and solidification conditions in order to examine their mechanical and physicochemical properties using modern methods. The chemical composition and microstructure of the alloys are the same as the original alloys; hence, it follows that the conclusion that the alloy properties are also comparable.

The simulation results showed that, in the case of bracelet making, porosity could be quite common. However, by modifying the process by changing the shape and length of the sprue and pouring cup as well as the mold, it is possible to change the porosity location in a way that does not affect the quality of the cast surfaces. The simulation showed that, for the crescent-shaped bracelet mold (inv. no. 182/77), the small cavity cross section could additionally interfere with the liquid metal filling the knobby ends. Heating the mold in this case could result in removing this porosity. The porosity scale is so low that defects should not be expected on the visible parts of the bracelets. In the case of the bracelet with the asymmetric ending (inv. no. 14/78), the gating system suggested by the "process engineers" from the Grzybiany settlement, together with heating the mold up to 600°C, could introduce porosity into other regions of the cast and scatter its shape. The gating system can also become the riser in this case; therefore, increasing its cross-section and steering can make the technological processes much easier.

The research suggests that the technology of investment casting into clay molds was mastered to the degree that ensured casts without defects. This conclusion comes from the observations of the MAGMA simulations for bracelet casting, which indicate common knowledge of some technical rules that were probably learned empirically in the Grzybiany settlement.

The research consisted of complex studies of artifacts, molds, and alloys from the very significant workshop in the Grzybiany settlement. As a result, it offers great insight into the mold-production technology and into the alloys and casts of the Bronze and Early Iron Ages.

The experiment of model alloys and application of the computer modeling methods need to be acknowledged as a serious direction in the development of the methodology development in the beginnings of bronze casting technology research.

REFERENCES

[1] B.S. Ottaway, Eur. J. Archaeol. **4** (1), 87-112 (2001).
[2] B.W. Roberts, Ch. Thornton (Eds.), Archaeometallurgy in Global Perspective Methods and Syntheses, Springer (2014).
[3] M.A.A. Khan, A.K. Sheikh, B.S. Al-Shaer, Evolution of Metal Casting Technologies. A Historical Perspective, Springer (2017).
[4] S.E. Greer, A comparison of the ancient metal casting materials and processes to modern metal casting materials and processes, Hartford, Connecticut: Master of Mechanical Engineering. Rensselaer Polytechnic Institute (2009).
[5] S. Pattnaik, D.B. Karunakar, P.K. Jha, J. Mater. Process. Tech. **212** (11), 2332-2348 (2012) DOI: 10.1016/j.jmatprotec.2012.06.003.
[6] E. Chica, S. Agudelo, N. Sierra, Renew. Energ. **60**, 739-745 (2013) DOI: 10.1016/j.renene.2013.06.030.
[7] R. Singh, S. Singh, M.S.J. Hashmi, Investment Casting, Reference Module in Materials Science and Materials Engineering (2016) DOI: 10.1016/B978-0-12-803581-8.04163-1.
[8] C. Cheah, C. Chua, C. Lee, et al. Int. J. Adv. Manuf. Technol. **25** (3-4), 308-320 (2005) DOI: 10.1007/s00170-003-1840-6.
[9] J. Aguilar, A. Schievenbusch, O. Kättlitz, Intermetallics **19** (6), 757-761 (2011). DOI: 10.1016/j.intermet.2010.11.014.
[10] K. Zaba, S. Nowak, M. Kwiatkowski, M. Nowosielski, P. Kita, A. Sioma, Arch. Metall. Mater. **59** (4), 1517-1525 (2015) DOI: 10.2478/amm-2014-0250.
[11] J. Cheng, T. Guo, J. Biomed. Eng. **15** (4), 414-418 (1998).
[12] S. Rzadkosz, J. Zych, A. Garbacz-Klempka, M. Kranc, J. Kozana, M. Piękoś, J. Kolczyk, Ł. Jamrozowicz, T. Stolarczyk, Metalurgija **54** (1), 293-296 (2015).
[13] A. Garbacz-Klempka, J.S. Suchy, Z. Kwak, T. Tokarski, R. Klempka, T. Stolarczyk, Study of investment casting technology from Bronze Age. Casting workshop in Grzybiany (southwest Poland), Arch. Metall. Mater. **63** (2), 615-624 (2918).
[14] A. Garbacz-Klempka, J. Kozana, M. Piękoś, Z. Kwak, P. Długosz, T. Stolarczyk, Archives of Foundry Engineering **15** (spec. iss. 1), 21-26 (2015).
[15] E. Pernicka, Provenance Determination of Archaeological Metal Objects, Archaeometallurgy in Global Perspective. Methods and

Syntheses, in: B.W. Roberts, Ch.P. Thornton (Eds.) Springer (2014).

[16] E. Ciliberto, G. Spoto, Modern analytical methods in art and archaeology. Toronto, (2000).

[17] A.M. Pollard, C.M. Batt, B. Stern, S.M.M. Young, Analytical chemistry in archaeology, Cambridge University Press (2007).

[18] M. Bos, J.A.M. Vrielink, Anal Chim Acta **373** (2-3), 291-302 (1998).

[19] T. Kearns, M. Martinón-Torres, T. Rehren, Historical Metallurgy **44** (1), 48-58 (2010).

[20] D. Dungworth, Historical Metallurgy **34** (2), 83-86 (2000).

[21] M. Pearce, STAR: Science & Technology of Archaeological Research **2** (1), 46-53 (2017). DOI: 10.1080/20548923.2016.1160593.

[22] M.S. Shackley, An Introduction to X-Ray Fluorescence (XRF) Analysis in Archaeology. In: Shackley M. (Eds.) X-Ray Fluorescence Spectrometry (XRF) in Geoarchaeology. Springer: New York, NY (2011). DOI: 10.1007/978-1-4419-6886-9_2.

[23] M. Lo Brutto, P. Meli, International Journal of Heritage in the Digital Era Article Information **1** (1), 1-6 (2012). DOI: 10.1260/2047-4970.1.0.1.

[24] A. Garbacz-Klempka, M. Szucki, Arch. Metall. Mater. **54** (2), 339-345 (2009).

[25] A. Garbacz-Klempka, Z. Kwak, P.L. Żak, M. Szucki, D. Ścibior, T. Stolarczyk, K. Nowak, Archives of Foundry Engineering **17** (3), 184-190 (2017).

[26] H.C. Miles, A.T. Wilson, F. Labrosse, B. Tiddeman, J.C. Roberts, Journal on Computing and Cultural Heritage **9** (1), 4:1-4:18 (2016). DOI: 10.1145/2795233.

[27] P. Reilly, IBM Systems Journal **28** (4), 569-579 (1989). DOI: 10.1147/sj.284.0569.